Journal of Cleaner Production 234 (2019) 549–558

Contents lists available at ScienceDirect

Journal of Cleaner Production

journal homepage: www.elsevier.com/locate/jclepro

Spatial-temporal characteristics of green travel behavior based on vector perspective

Wenbin Zhang [a, b], Zihao Tian [c, *], Guangyong Zhang [a], Gaogao Dong [a]

[a] Energy Development and Environmental Protection Strategy Research Center, Jiangsu University, Zhenjiang, 212013, Jiangsu, China
[b] Department of Mathematical Science, Nanjing University of Science & Technology, Taizhou Institute of Science & Technology, Taizhou, 225300, Jiangsu, China
[c] School of Management & Engineering, Nanjing University, Nanjing, 210094, Jiangsu, China

ARTICLE INFO

Article history:
Received 14 February 2019
Received in revised form
12 April 2019
Accepted 12 June 2019
Available online 14 June 2019

Handling editor: Yutao Wang

Keywords:
Green travel behavior
Vector perspective
Spatial-temporal characteristics
Coarse graining method
Temporal network

ABSTRACT

In this paper, the spatial-temporal characteristics of green travel behavior in public bike-sharing system are studied. From the vector perspective, a coarse graining method of green travel direction is proposed, the methods and steps of analyzing the spatial characteristics and temporal window of green travel behavior are established, which opens up new horizons in the study of green travel behavior, develop the existing coarse granulation methods and temporal network theory, and provides a new way of route optimization and high-frequency task window recognition for the dynamic rebalancing scheme. At the same time, we conduct an empirical analysis by the travel data of the public bike-sharing system in Nanjing from March 20, 2017 to March 26, 2017, and verify the dynamic spatial characteristics and time-varying of green travel behavior based on vector perspective.

1. Introduction

As a sustainable, efficient, economical, flexible and environmentally friendly transportation mode, public bike has become an increasingly powerful way to alleviate the last-mile problem. Around the world, public bike-sharing system has been operated in about 1500 cities at present (Ahmadreza et al., 2017; Haider et al., 2018), and green travel behavior has been widely concerned by scholars (Si et al., 2019).

Travel data records green travel behavior in time and space, and contains a large amount of potentially valuable information. The improvement of data acquisition and analysis of public bike system promotes the research of green travel behavior. In order to capture the characteristics of green travel behavior, travel speed (Jensen et al., 2010), travel time (Jappinen et al., 2013), the gendered travel behavior (Zhao et al., 2015), travel type (Bordagaray et al., 2016), trip chains (Zhang et al., 2018) and spatial structure (Boss et al., 2018) are studied. At the same time, the relationships between green travel behavior and site selection (Wang et al., 2016), the sustainability and efficient functioning of cities (Bullock et al., 2017), dynamic repositioning (Zhang et al., 2017), built environments (Liu and Lin, 2019), job accessibility (Pritcharda et al., 2019) are analyzed according to the spatial-temporal characteristics of the data.

Spatial-temporal characteristics are the eternal research theme of the objective world. Although there are many literatures on green travel behavior, the researches focus on spatial-temporal characteristics by travel data are limited, and there are some imperfections: 1) spatial characteristics are mostly based on statistical pattern (Zhao et al., 2015; Wang et al., 2016; Zhang et al., 2018; Boss et al., 2018), and lack of dynamic analysis from the vector perspective; 2) temporal characteristics are mostly based on artificial time windows with equal intervals (Wang et al., 2016; Bordagaray et al., 2016; Pritcharda et al., 2019), and lack of high frequency temporal windows which are based on dynamic spatial characteristics to describe green travel behavior with tidal phenomena (Chardon et al., 2016).

To fill this gap, we will establish a new vector coarse graining method and construct a directional index of spatial characteristics, and analyze the dynamic spatial-temporal characteristics of green

* Corresponding author.
E-mail address: swytzh@hotmail.com (Z. Tian).

https://doi.org/10.1016/j.jclepro.2019.06.132
0959-6526/

travel behavior in the vector field established by temporal network. It will open up new horizons for the study of green travel behavior, the route optimization and the identification of high-frequency task windows in the dynamic rebalancing scheme, and be a powerful complement to existing coarse granulation methods (Wang et al., 2016a; Wang et al., 2018) and complex network theory (Dong et al, 2012; Wang et al., 2016b; Dong et al., 2018).

The scheme of green travel behavior's spatial-temporal characteristics in this paper is shown in Fig. 1, and the remainder of the paper is organized as follows: Section 2 reviews the relevant literature. Section 3 provides the new methods and symbols. Section 4 carries out empirical analysis.

2. Literature review

The research on green travel behavior is rich. According to the content, existing literature can be divided into two categories. One focus on the factors that influence green travel behavior, such as the sign-up process (Fishman et al., 2012), topography (Iderlina et al., 2016), weather (Mattson and Godavarthy, 2017; Godavarthy and Taleqani, 2017), public bike infrastructure (Chardon et al., 2017; Hamilton and Wichman, 2018), and Convenience (Fishman et al., 2014; Si et al., 2019).

The other is the rebalancing problem. According to static and dynamic rebalancing models, minimizing the total unmet demand (Contardo et al., 2012; Chemla et al., 2013; Szeto et al., 2016; Shui and Szeto, 2018) and minimizing vehicle travel time or cost (Benchimol et al., 2011; Dell'Amico et al., 2014; Kloimllner et al., 2014; Pfrommer et al., 2014; Rainer-Harbach et al., 2015; Schuijbroek et al., 2017; Zhang et al., 2017) are analyzed.

In addition, some studies have confirmed that green travel behavior can indeed improve traffic flow (Wang and Zhou, 2017; Hamilton and Wichman, 2018) and improve people's health (Fuller et al., 2013; Ricci, 2015). The necessity of wearing helmet has also been confirmed (Graves et al., 2014).

3. New methods and symbols

3.1. Two network of green travel behavior

To describe the behavior of borrowing public bike and returning public bike, we introduce two complex networks.

Definition 1. 1) In the interval $[t, t+\Delta t]$, we represent the stations of the public bike-sharing system as nodes $\{V\}_{i=1}^{N}$, the borrowed record from station V_i to station V_j as a directed edge E_{ij}, and the number of borrowed public bikes between the station V_i and station V_j as a weight w_{ij} to establish a directed and weighted complex network of borrowing public bike behavior, and record it as $G_B(V, E)$.

2) In the interval $[t, t+\Delta t]$, we represent the station of the public bike-sharing system as a node $\{V\}_{i=1}^{N}$, the returned record from station V_j to station V_i as a directed edge E_{ji}, and the number of returned public bikes between the station V_j and station V_i as a weight w_{ji} to establish a directed and weighted complex network of returning public bike behavior, and record it as $G_R(V, E)$.

3.2. Spatial characteristic

Since vector can describe the spatial distribution of green travel behavior from quantity and direction, we will establish a vector coarse graining method to construct the spatial characteristics of green travel behavior.

3.2.1. Vector representation of node flow

In the public bike network (PBN), the number and direction of borrowed and returned public bikes on the nodes well describe the public travel behavior on the corresponding stations. Therefore, we refer to the number and direction of borrowed and returned public bikes on the node as the outflow and inflow of the node, collectively referred to as the flow of the node. And we introduce the following definitions.

Definition 2. 1) Let $\{V\}_{i=1}^{N}$ be the nodes of $G_B(V, E)$, w_{ij} be the weight on the directed edge E_{ij}, then vector $[w_{i1}, w_{i2}, \cdots, w_{iN}]$ represents the outflow of node V_i, and we record it as V_i^{out}. At the same time, we record the j-th sub-vector of V_i^{out} on the directed edge E_{ij} is $\vec{E}_{ij}$, where $\vec{E}_{ij} = w_{ij} \cdot \vec{E}_{ij}^{0}$, $\vec{E}_{ij}^{0}$ indicating the unit direction of the directed edge E_{ij}, $1 \le i, j \le N$;

2) Let $\{V\}_{i=1}^{N}$ be the nodes of $G_R(V, E)$, w_{ij} be the weight on the directed edge E_{ij}, then vector $[w_{1i}, w_{2i}, \cdots, w_{Ni}]$ represents the inflow of node V_i, we record it as V_i^{in}. And we record the j-th sub-vector of V_i^{in} on the directed edge E_{ji} is $\vec{E}_{ji}$, where $\vec{E}_{ji} = w_{ji} \cdot \vec{E}_{ji}^{0}$, $\vec{E}_{ji}^{0}$ indicating the unit direction of the directed edge E_{ji}, $1 \le i, j \le N$.

Note 1. Although $\sum_j \vec{E}_{ij} = [w_{i1}, w_{i2}, \cdots, w_{iN}] \cdot [\vec{E}_{i1}^{0}, \vec{E}_{i2}^{0}, \cdots, \vec{E}_{iN}^{0}]$ is a linear representation of V_i^{out}, and $\sum_j \vec{E}_{ji} = [w_{1i}, w_{2i}, \cdots, w_{Ni}] \cdot [\vec{E}_{1i}^{0}, \vec{E}_{2i}^{0}, \cdots, \vec{E}_{Ni}^{0}]$ is a linear representation of V_i^{in}, but they are no practical significance in PBN.

For example, $G_B(V, E)$ is a B-PBN, and there are three public bikes borrowed from node V_1, two go to node V_2 and the other one to node V_3. Then there are two cases of the outflow vector $V_1^{out} = \vec{E}_{12} + \vec{E}_{13}$ (See Fig. 2).

In Fig. 2 (a), $\vec{E}_{12} + \vec{E}_{13}$ does not point to any one of the nodes $\{V_i\}_{i=1}^{4}$ in $G_B(V, E)$. That is, the borrowed public bikes from node V_1 do not go to the nodes $\{V_i\}_{i=1}^{4}$ in $G_B(V, E)$. Then the vector $\vec{E}_{12} + \vec{E}_{13}$ has no practical meaning. In Fig. 2 (b), $\vec{E}_{12} + \vec{E}_{13}$ point to node V_4 in $G_B(V, E)$. In fact, none of the borrowed public bikes from node V_1 will go to node V_4. Therefore, the vector $\vec{E}_{12} + \vec{E}_{13}$ still has no practical meaning.

3.2.2. Vector coarse graining method

The dominant directional component (DDC) in the vector (Almaas et al., 2004) can effectively describe the overall trend of outflow and inflow of the node, and reveal the preference of green travel behavior. Based on the different cases of DDC, we construct a new coarse graining method for vectors.

Definition 3. Let $V = [a_1, a_2, \cdots, a_n] \neq 0$, $\vec{E}_i^{0}$ be the unit vector of the i-th sub-vector in V, $i = 1, 2, \cdots, n$. If there is a a_i satisfies:

$$|a_i| \ge \frac{1}{2}|V| \tag{1}$$

Then the vector V has a unique dominant sub-vector $a_i \cdot \vec{E}_i^{0}$.

For example, $[0, 2, 1]$ is the outflow V_1^{out} of node V_1 on $G_B(V, E)$ (See, Fig. 3), the total number of borrowed public bikes on node V_1

is $|V_1^{out}| = |\overrightarrow{E}_{11}| + |\overrightarrow{E}_{12}| + |\overrightarrow{E}_{13}| = w_{11} + w_{12} + w_{13} = 3$, and the number of borrowed public bikes on the sub-vector $\overrightarrow{E}_{12}$ is $|\overrightarrow{E}_{12}| = w_{12} = 2 > \frac{3}{2}$ (See, Fig. 3(a)). Then, the sub-vector $\overrightarrow{E}_{12}$ represents 66.67% of the outflow V_1^{out} on node V_1, which portrays the overall trend of the outflow V_1^{out}, and is the dominant sub-vector in V_1^{out} (See, Fig. 3(b)).

Generally, according to the number of dominant sub-vectors in the vector, we establish the following coarse graining method.

Definition 4. Let $V = [a_1, a_2, \cdots, a_n] \neq 0$, $\{|\tilde{a}_i|\}_{i=1}^n$ is the new sequence reordered from small to large by sub-vector weights $\{|a_i|\}_{i=1}^n$, where $|\tilde{a}_1| \geq |\tilde{a}_2| \geq \cdots \geq |\tilde{a}_n|$. $A_1, A_2, \cdots, A_k$ is the k sets obtained by classifying the elements in $\{|\tilde{a}_i|\}_{i=1}^n$ according to the law of numerical equality (i.e. let $\tilde{a}_i \in A_i$, $\tilde{a}_j \in A_j$ $(i > j)$, then $|\tilde{a}_i| \equiv c_i$, $|\tilde{a}_j| \equiv c_j$, and $|\tilde{a}_i| \geq |\tilde{a}_j|$). If there is a positive integer $h(\geq 1)$, the following conditions are met:

$$\sum_{\tilde{a}_i \in \cup_{i=1}^{h} A_i} |\tilde{a}_i| \geq \frac{1}{2}|V|, \text{ and } \sum_{\tilde{a}_i \in \cup_{i=1}^{h-1} A_i} |\tilde{a}_i| < \frac{1}{2}|V|, \ h \leq k. \tag{2}$$

Let m is the number of elements in the set $\cup_{i=1}^{h} A_h$, then the number of dominant sub-vectors in V is m, and the vector V is called m-type coarse graining vector, which is denoted as ${}^mV$.

In Fig. 3., for example, $\overrightarrow{E}_{12}$, $\overrightarrow{E}_{13}$ is the non-zero sub-vectors of the outflow V_1^{out}, and $|\overrightarrow{E}_{12}| = 2$, $|\overrightarrow{E}_{13}| = 1$, $|V| = 3$ and. Then $|\overrightarrow{E}_{12}| > \frac{1}{2}|V|$, and $m = 1$. That is, V_1^{out} is a 1-type coarse graining vector.

3.2.3. Coarse graining method of node flow

Applying the above conclusions to the directional weighted complex network, we obtain the coarse granulation method of the node flow as follows.

Theorem 1. *Let V_i be a node in the directed and weighted complex network $G(V, E)$, V_i^{out}, V_i^{in} respectively represent the outflow and inflow on node V_i, and w_{ij} be the weight on the directed edge E_{ij}, $1 \leq i, j \leq N$.*

1) If the number of dominant sub-vectors of the outflow V_i^{out} is m, then node outflow V_i^{out} is a m-type coarse graining vector, which is recorded ${}^mV_i^{out}$;
2) If the number of dominant sub-vectors in the inflow V_i^{in} is m, then node inflow V_i^{in} is a m-type coarse graining vector, which is recorded ${}^mV_i^{in}$.

For convenience, we introduce the coarse-graining characteristic function of the outflow and inflow on node V_i in the directed and weighted complex network $G(V, E)$ as follows:

$${}^m y_i^{out} = \begin{cases} 1, & if \ V_i^{out} \in {}^mV_i^{out}, \\ 0, & other \end{cases} \tag{3}$$

and

$${}^m y_i^{in} = \begin{cases} 1, & if \ V_i^{in} \in {}^mV_i^{in}, \\ 0, & other. \end{cases} \tag{4}$$

3.2.4. Directional degree of directed and weighted networks

The coarse graining method of node flow simplifies the edges in the directed and weighted network, which is effective to explore the law among node flow in network, and to depict spatial characteristics of green travel behavior. To further characterize green travel behavior, we introduce directional degree of the directed and weighted network as follows:

Definition 5. Let V_i be an node in the directed and weighted complex network $G(V,E)$, and let V_i^{out}, V_i^{in} be the outflow and inflow on node V_i, $i = 1, 2, \cdots, N$.

$${}^mY^{out} = \frac{\sum_i y_i^{out}}{\sum_i \mathrm{sgn}\left(s_i^{out}\right)}, \tag{5}$$

where s_i^{out} is the out strength on node V_i and $\mathrm{sgn}(x)$ is the sign function;

$${}^mY^{in} = \frac{\sum_i y_i^{in}}{\sum_i \mathrm{sgn}\left(s_i^{in}\right)}, \tag{6}$$

where s_i^{in} is the in strength on node V_i and $\mathrm{sgn}(x)$ is the sign function.

1) After node outflow $\{V_i^{out}\}_{i=1}^N$ is processed by the coarse graining method, the ratio of m-type coarse graining vector ${}^mV_i^{out}$ is called m-type outflow directional degree of the directed and weighted network $G(V,E)$, and it is recorded as ${}^mY^{out}$:
2) After node inflow $\{V_i^{in}\}_{i=1}^N$ is processed by the coarse graining method, the ratio of m-type coarse graining vector ${}^mV_i^{in}$ is called m-type inflow directional degree of the directed and weighted network $G(V,E)$, and it is recorded as ${}^mY^{in}$:

In complex network $G(V,E)$ (See, Fig. 4), for example, $\overrightarrow{E}_{12}$, $\overrightarrow{E}_{22}$, $\overrightarrow{E}_{32}$ are the dominant sub-vectors of the outflow on the nodes $\{V\}_{i=1}^3$ respectively. $\overrightarrow{E}_{12}$, $\overrightarrow{E}_{22}$, $\overrightarrow{E}_{32}$ constitute a new vector field (See, Fig. 4 (b)), which represents more than half of the node outflow in the entire network and portrays the overall spatial characteristics of the network. Similarly, $\overrightarrow{E}_{31}$, $\overrightarrow{E}_{12}$, $\overrightarrow{E}_{13}$ are the dominant sub-vectors of the inflow on the nodes $\{V\}_{i=1}^3$ respectively, and they form another new vector field (Fig. 4 (c)), which represents more than half of the node inflow in the whole network and characterizes the overall spatial characteristics of the network.

3.3. Temporal characteristic

Green travel behavior is time-varying. In different time windows, the value of directional degree is different. Temporal network is an effective tool for portraying the timeliness of the behavior. Therefore, we describe temporal characteristics of green travel behavior by temporal windows.

3.3.1. Standard of temporal window division

Based on the analysis of directional degree, we establish the following criteria for dividing temporal windows:

Definition 6. 1) Let $[t_B, t_E]$ be the time interval of borrowed records, $\{[t^\alpha, t^\alpha + \Delta t^\alpha]\}_{\alpha=1}^N$ is any non-overlapping temporal windows

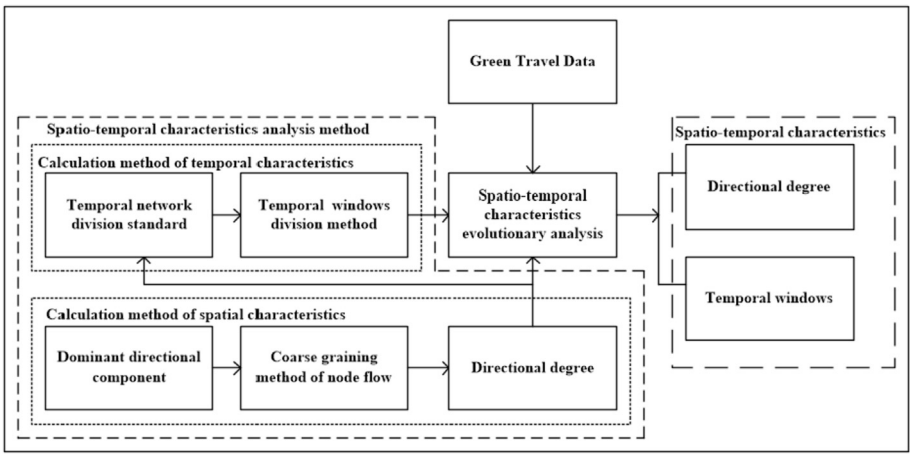

Fig. 1. Spatial-temporal characteristics analysis method of green travel behavior.

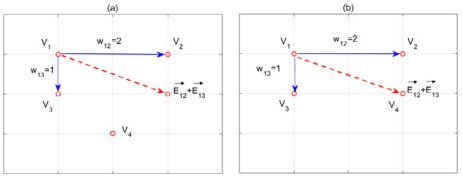

Fig. 2. Two cases of the node outflow V_1^{out} by vector addition.

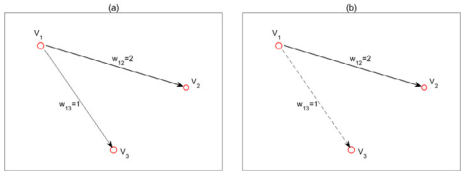

Fig. 3. The outflow of node V_1.

division on $[t_B, t_E]$, and $\{G^\alpha(V^\alpha, E^\alpha)\}_{\alpha=1}^N$ is the corresponding temporal network. If the k-type outflow directional degree in temporal network satisfies:

$$\min_\alpha \sum_{k=1}^m {}^kY^{\alpha,out} \geq c_1. \tag{7}$$

Then, $\{[t^\alpha, t^\alpha + \Delta t^\alpha]\}_{\alpha=1}^N$ is called a m-type valid division on the time interval $[t_B, t_E]$ under the parameter c_1, and c_1 is temporal factor in B-PBN.

$$\min_\alpha \sum_{k=1}^m {}^kY^{\alpha,in} \geq c_2. \tag{8}$$

2) Let $[t_B, t_E]$ be the time interval of returned records, $\{[t^\alpha, t^\alpha + \Delta t^\alpha]\}_{\alpha=1}^N$ is any non-overlapping temporal windows division on $[t_B, t_E]$, and $\{G^\alpha(V^\alpha, E^\alpha)\}_{\alpha=1}^N$ is the corresponding temporal network. If the k-type inflow directional degree in temporal network satisfies:

Then, $\{[t^\alpha, t^\alpha + \Delta t^\alpha]\}_{\alpha=1}^N$ is called a m-type valid division on the time interval $[t_B, t_E]$ under the parameters c_2, and c_2 is temporal factor in R-PBN.

Note 2. The factors c_1 and $c_2 (\in [0, 1])$ characterize the minimum of the m-type directional degree within temporal windows, reflect the overall worst level of spatial characteristic.

Note 3. It can be seen from the Definition 3 that the spatial characteristic on the node which has the 1-type coarse graining vector is more obvious. Then, the value of the 1-type direction degree under temporal windows is higher, the edges in the network by coarse graining method is fewer. Therefore, we will obtain temporal windows by the 1-type valid division in this paper.

3.3.2. Methods of temporal window division

Now, we propose a method for dividing temporal windows, as follow:

Definition 7. 1) Given temporal factor c_1 of $G_B(V, E)$, and take $\Delta t^\alpha = t^\alpha - t^{\alpha-1} \equiv C(>0)$ to divide $[t_B, t_E]$ into equal time interval : $T_B = t^0 < t^1 < t^2 < \cdots < t^\alpha < \cdots < t^{N-1} < t^N = T_E$. If $\{[t^\alpha, t^\alpha + \Delta t^\alpha]\}_{\alpha=1}^N$ is a m-type valid division, then we called $\min_{\Delta t^\alpha}\{[t^\alpha, t^\alpha + \Delta t^\alpha]\}_{\alpha=1}^N$ is a m-type temporal windows of $G_B(V, E)$ under temporal factor c_1;

2) Given temporal factor c_2 of $G_R(V, E)$, and take $\Delta t^\alpha = t^\alpha - t^{\alpha-1} \equiv C(>0)$ to divide $[t_B, t_E]$ into equal time interval: $T_B = t^0 < t^1 < t^2 < \cdots < t^\alpha < \cdots < t^{N-1} < t^N = T_E$. If $\{[t^\alpha, t^\alpha + \Delta t^\alpha]\}_{\alpha=1}^N$ is a m-type valid division, then we called $\min_{\Delta t^\alpha}\{[t^\alpha, t^\alpha + \Delta t^\alpha]\}_{\alpha=1}^N$ is a m-type temporal windows of $G_R(V, E)$ under temporal factor c_2.

For example, according to the borrowed records in Table 1, we establish a complex network $G_B(V, E)$ (See, Fig. 5 (a)) and build a temporal network $\{G_B^\alpha(V^\alpha, E^\alpha)\}_{\alpha=1}^2$(See, Fig. 5 (b)-(c)) by two equal time intervals. According to Definition 5, we calculate 1-type directional degree of each network (See, Fig. 5 (d)-(i)).

In network $G_B(V, E)$ (See, Fig. 5 (a)), ${}^1Y^{out}$ is 1/3 (See, Fig. 5 (d)), and ${}^1Y^{in}$ is 1/3 (See, Fig. 5 (g)) under window $[t_1, t_8]$. In $G_B^1(V^1, E^1)$ (See, Fig. 5 (b)), ${}^1Y^{1,out}$ is 1 (See, Fig. 5 (e)), and ${}^1Y^{1,in}$ is 1 (See, Fig. 5 (h)) under temporal window $[t_1, t_4]$. In $G_B^2(V^2, E^2)$. ${}^1Y^{2,out}$ is 1 (See, Fig. 5 (f)), and ${}^1Y^{2,in}$ is 1 (See, Fig. 5 (i)) under temporal window $[t_5, t_8]$. According to Definition 6, $\{[t_1, t_4], [t_5, t_8]\}$ is a valid division on the time interval $[t_1, t_8]$.

It can be seen that green travel behavior in the public bike-sharing system is closely related to temporal windows, and

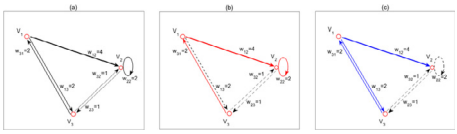

Fig. 4. The node flow of the complex network.

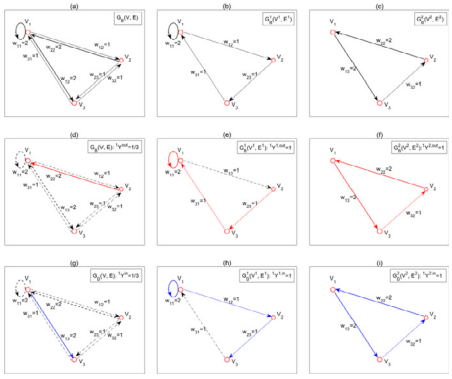

Fig. 5. Networks and their 1-type directional degrees.

temporal windows is more conducive to the mining of the spatial-temporal characteristic of green travel behavior. Therefore, we can obtain the high-frequency temporal windows by numerical evolution analysis of the 1-type directional degree in temporal network.

4. Empirical analysis

4.1. Data

In this paper, 940,368 borrowed records and 940,421 returned records are the real-time records of Nanjing public bike company from march 20, 2017 to march 26 2017. We fix time interval as 20, 10, 5, 2 and 1 min respectively, and obtain the frequency of borrowed records and returned records in each group of time intervals (See, Fig. 6). In this paper, MATLAB is used to calculate and plot.

The daily frequency distributions of borrowed records (See, Fig. 6 (a)) and returned records (See, Fig. 6 (b)) of green travel behavior are very uneven, showing a distinct 'tidal wave' phenomenon: at 0:00–6:00 before dawn, the frequency is very small; in the morning peak 7:00–10:00 and the evening peak 17:00–20:00, the frequency increases sharply, and presents tidal phenomenon (Affected by the arrival of rainfall, tidal phenomenon does not appear in the evening peak on Wednesday), and the tidal phenomenon on weekdays is more obvious than the weekend; the frequency at other times is relatively stable. At the same time, the above-mentioned 'tidal' phenomenon does not depend on the time interval. Therefore, the public travel behavior is time-varying, and does not depend on time interval, which is an inherent attribute of the public bike-sharing system. Therefore, the spatial-temporal characteristics of green travel behavior in different temporal windows need to be treated differently.

4.2. Spatial-temporal characteristics of green travel behavior

Since the methods of m-type directional degree and m-type temporal window are fixed, we will only analyze the spatial-temporal characteristics with 1-type directionality and 1-type temporal window.

4.2.1. Evolution analysis of spatial-temporal characteristics

In this section, we take five fixed values as the time interval, establish five sets of temporal networks, and analyze spatial-temporal characteristics of green travel behavior by 1-type directional degree under each temporal window.

4.2.1.1. Green travel behavior of borrowing public bike. Taking 20 as the time interval Δt_α (minute), 504 temporal windows are obtained. According to borrowed records in each temporal window, we establish the temporal networks and calculated the values of 1-type out directional degree ${}^1Y^{\alpha,\ out}$ by formula (3) and (5).

Fixed Δt_α as 10, 5, 2 and 1, borrowed records are divided into 1008, 2016, 5040 and 10,080 temporal windows respectively, and the value of ${}^1Y^{\alpha,\ out}$ under each temporal window is calculated as shown in Fig. 7 (b)-(e).

We find that ${}^1Y^{\alpha,\ out}$ is time-varying, and its value is closely related to frequency (Fig. 7): during the morning peak 7:00–10:00 and the evening peak 17:00–20:00, the frequency is the highest,

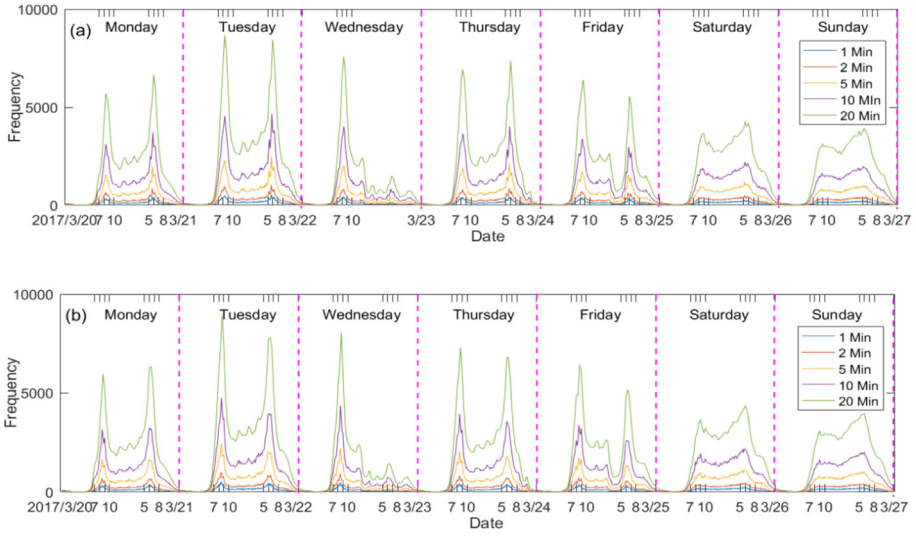

Fig. 6. Borrowed records frequency and returned records frequency.

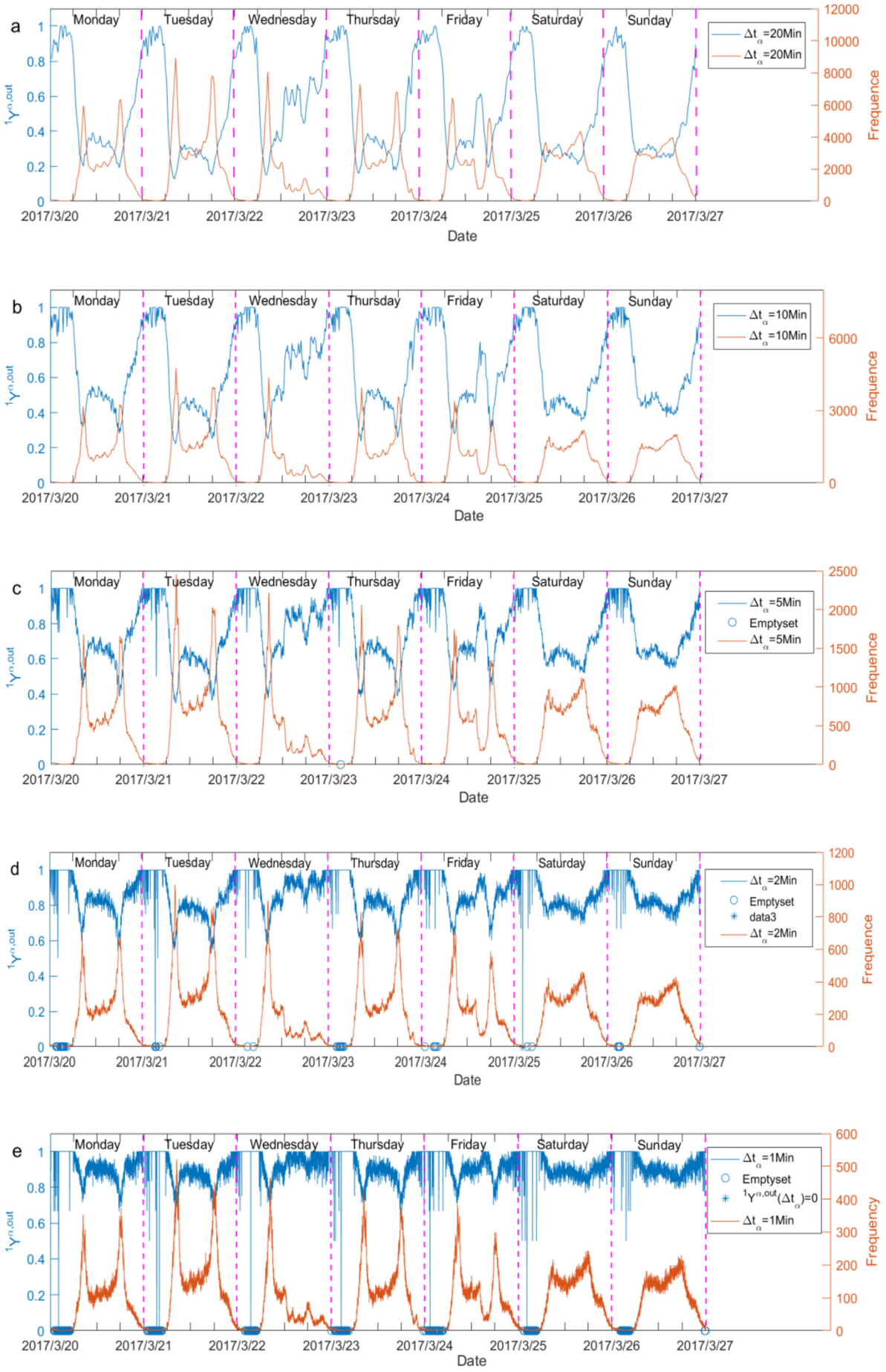

Fig. 7. 1-type outflow directional degree and borrowed records frequency under different time intervals.

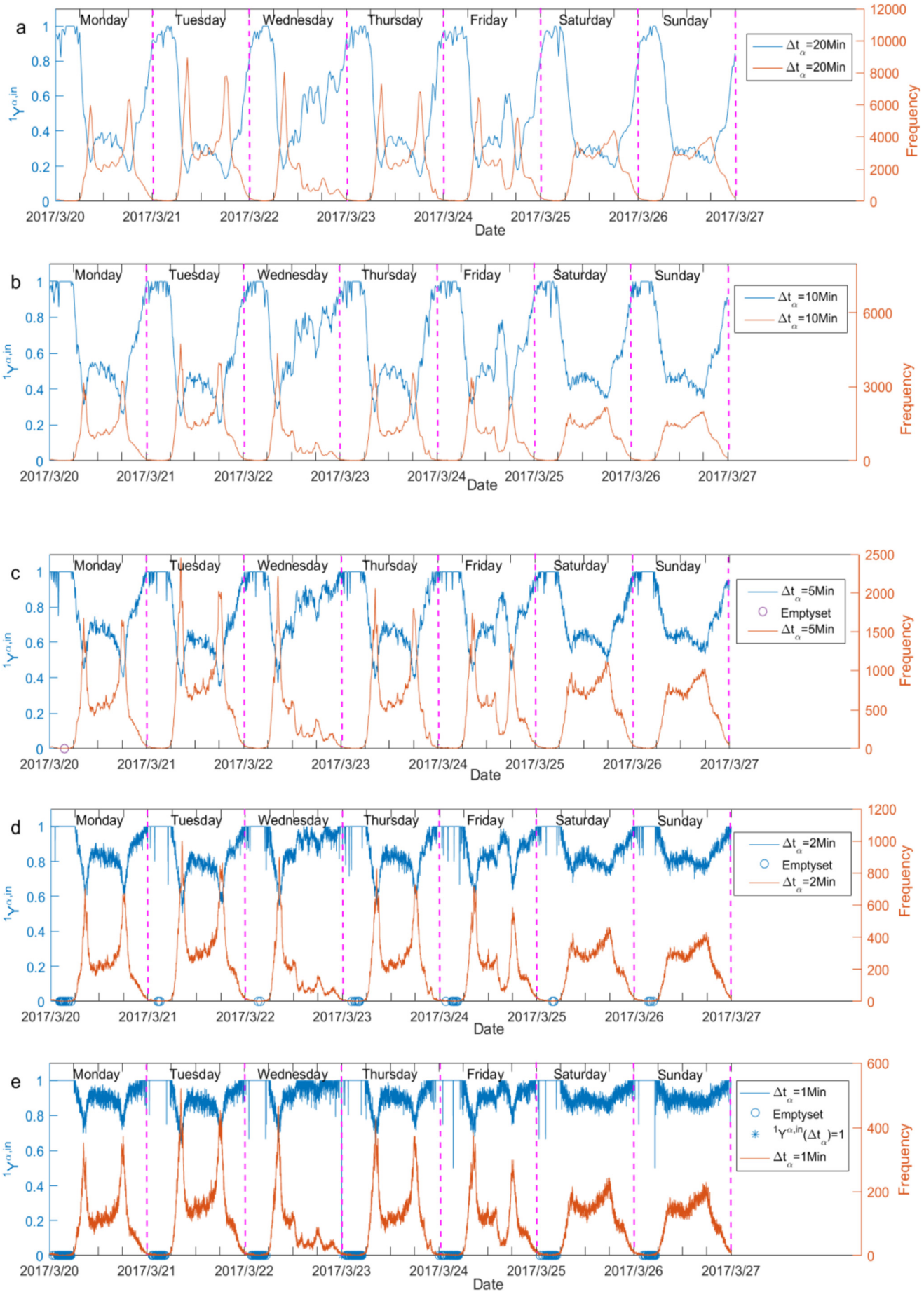

Fig. 8. 1-type inflow directional degree and returned records frequency under different time intervals.

and the average value of ${}^1Y^{\alpha,\ out}$ at different temporal windows is the smallest, 0.3430, 0.4792, 0.6211, 0.7794 and 0.8628, respectively; during 0:00–6:00 before dawn, the frequency is the least, and the average value of ${}^1Y^{\alpha,\ out}$ at different temporal windows is the highest, reaching 0.9284, 0.9561, 0.9706, 0.9462 and 0.8605 respectively; during the other three periods 6:00–7:00, 10:00–17:00 and 20:00–24:00, the frequency is moderate, and the average value of at different time intervals is second, 0.5378, 0.6662, 0.7800, 0.8856 and 0.9329, respectively.

Comparing the effects of different time intervals on the spatial characteristics of borrowing public bike behavior (See, Fig. 7), we find that:

1) Between 6:00 and 24:00 after dawn, as the value of Δt^α decreases: 20 → 10 → 5 → 2 → 1, ${}^1Y^{\alpha,\ out}$ increases continuously: 0.1968 → 0.2866 → 0.4069 → 0.5561 → 0.6519. So, ${}^1Y^{\alpha,\ out} \propto \frac{1}{\Delta t^\alpha}$. That is, in the temporal network of borrowing public bike behavior during 6:00–24:00, the smaller the value of Δt^α, the more obvious the overall spatial characteristics under temporal windows.
2) Between 0:00 and 6:00 before dawn, as the value of Δt^α decreases, ${}^1Y^{\alpha,\ out}$ undergoes a process of rising and then decreasing, and its minimum values are: 0.7688 → 0.8333 → 0.500 → 0 → 0. At the same time, empty temporal windows that do not contain any records gradually appear: 0 → 0 → 1 → 49 → 331, and the temporal window with ${}^1Y^{\alpha,\ out} = 0$ is also increasing: 0 → 0 → 0 → 2 → 7 (See, Fig. 8), which breaking the law of ${}^1Y^{\alpha,\ out} \propto \frac{1}{\Delta t^\alpha}$. It meanings that, in the temporal network of borrowing public bike behavior during 0:00–6:00, the overall spatial characteristics are complicated with the value of Δt^α, which is not a simple linear relationship.

4.2.1.2. Green travel behavior of returning public bike. Fixed Δt_α as 20, 10, 5, 2 and 1, returned records are divided into 504, 1008, 2016, 5040 and 10,080 temporal windows respectively, and the value of ${}^1Y^{\alpha,\ in}$ under each temporal window is calculated as shown in Fig. 8.

We find that ${}^1Y^{\alpha,\ in}$ is also time-varying, and its value is closely related to frequency (Fig. 8): during 0:00–6:00 with the least frequency, the average value of ${}^1Y^{\alpha,\ in}$ under temporal windows is the highest, reaching 0.9465, 0.9700, 0.9852, 0.9526 and 0.8571 respectively; during 7:00–10:00 and 17:00–20:00 with the highest returned records frequency, the average value of ${}^1Y^{\alpha,\ in}$ under temporal windows is the smallest, which is 0.2943, 0.4375, 0.5913, 0.7633 and 0.8541, respectively; during the other three time periods 6:00–7:00, 10:00–17:00 and 20:00–24:00 with moderate returned records frequency, the average value of ${}^1Y^{\alpha,\ in}$ under temporal windows is second, which is 0.5238, 0.6590, 0.7788, 0.8882 and 0.9367, respectively.

Comparing the effects of different time intervals on the spatial characteristics of returning public bike behavior (See, Fig. 8), we find that:

1) Between 6:00 and 24:00 after dawn, as the value of Δt^α decreases: 20 → 10 → 5 → 2 → 1, ${}^1Y^{\alpha,\ in}$ increases continuously: 0.1281 → 0.2052 → 0.3485 → 0.5034 → 0.6372. So, ${}^1Y^{\alpha,\ in} \propto \frac{1}{\Delta t^\alpha}$. That is, in the temporal network of returning public bike behavior between 6:00 and 24:00, the smaller the value of Δt^α, the more obvious the overall spatial characteristics of returning public bike under temporal windows.
2) Between 0:00 and 6:00 before dawn, as the value of Δt^α decreases, ${}^1Y^{\alpha,\ in}$ undergoes a process of rising and then decreasing, and its minimum values are: 0.8143 → 0.8000 → 0.7500 → 0 → 0. At the same time, empty temporal windows that do not contain any records gradually appear: 0 → 0 → 1 → 51 → 352, and the temporal window with ${}^1Y^{\alpha,\ in} = 0$ is also increasing: 0 → 0 → 0 → 2 → 7 (See, Fig. 8), which breaking the law of ${}^1Y^{\alpha,\ in} = 0 \propto \frac{1}{\Delta t^\alpha}$. That is, in the temporal network of returning public bike behavior between 0:00 and 6:00, the overall spatial characteristics are complicated with the value of Δt^α.

To sum up, green travel behavior is time-varying, its spatial characteristic has a complex relationship with time interval Δt^α, and it should be treated differently according to six different periods (0:00–6:00, 6:00–7:00, 7:00–10:00, 10:00–17:00, 17:00–20:00 and 20:00–24:00).

4.2.2. Spatial-temporal characteristics

In this section, we calculate the spatial-temporal characteristics of green travel behavior in the above six different time intervals. At the same time, in order to ensure that spatial characteristic can represent the behavior of most green travelers, we set the temporal factors $c_1, c_2 \geq 0.6$.

After multiple evolutionary analysis, we obtain spatial-temporal characteristics of green travel behavior according to definitions 6 and 7 (See, Fig. 9), and the key parameters in each temporal window are sorted out (See, Table 2).

In terms of spatial characteristics, although the daily green travel behavior of borrowing public bike and returning public bike are different, the amplitudes of ${}^1Y^{\alpha,\ out}$ and ${}^1Y^{\alpha,\ in}$ are smaller and fluctuate around 0.8 all the time (See, Fig. 9). At the same time, there are no empty windows that do not contain any records. That is, green travel behavior has inherent spatial characteristics, and the characteristics be described by temporal windows and directional degree.

In terms of temporal characteristics, green travel behavior of borrowing public bike and returning public bike are consistency. In 5 time intervals: 0:00–6:00, 6:00–7:00, 10:00–17:00, 17:00–20:00 and 20:00–24:00, the temporal windows is the same. During the 3 h from 7:00 to 10:00, Δt^α of $G_B(V,E)$ is slightly larger than $G_R(V,E)$, which is 2 and 1 min respectively. According Definition 7, the 2 min is also a valid window division interval of $G_R(V,E)$ in 7:00–10:00. That is, in 6 time intervals: 0:00–6:00, 6:00–7:00, 7:00–10:00, 10:00–17:00, 17:00–20:00 and 20:00–24:00, Δt^α of green travel behavior can be unified: 120, 5, 2, 2.5, 1 and 0.66.

Therefore, we can analyze green travel behavior of borrowing public bike and returning behavior under the same high-frequency temporal windows. That is, the high-frequency temporal windows of green travel behavior can be used as the high-frequency task window of the dynamic rebalancing, and the calculation method provides a new idea for the identification of the high-frequency task window. At the same time, the coarse graining method of the node flow under the temporal windows also opens up new horizons for the route optimization of the dynamic rebalancing.

5. Conclusion

From a vector perspective, this paper establishes a new method and step to analyze and calculate the spatial-temporal characteristics of green travel behavior. Firstly, we establish a coarse grained

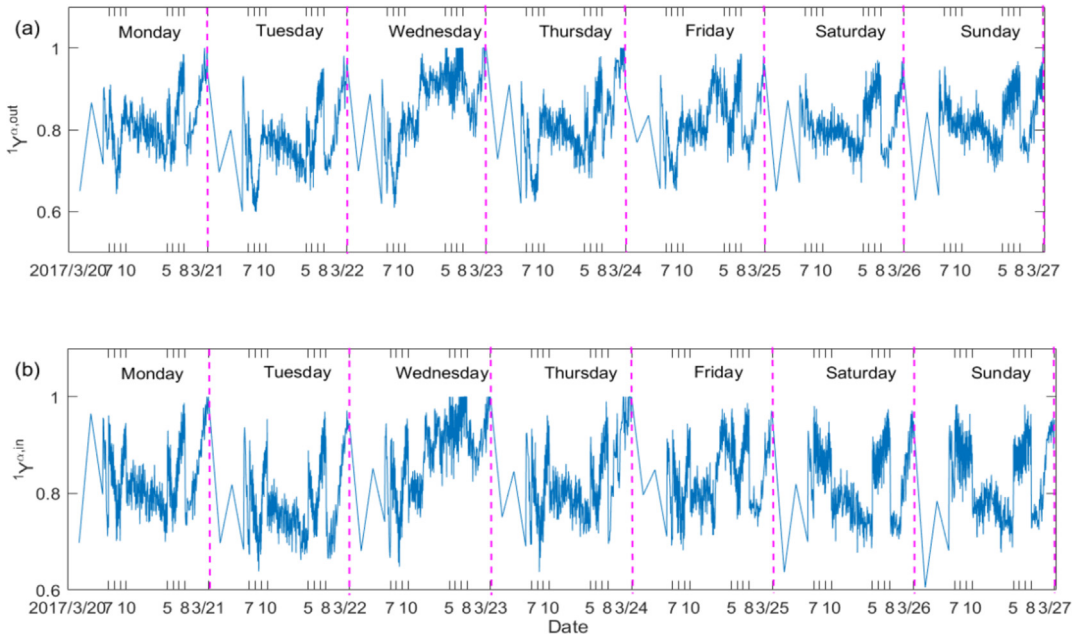

Fig. 9. Spatial-temporal characteristics of green travel behavior.

Table 1
Borrowed records of the public bike-sharing system.

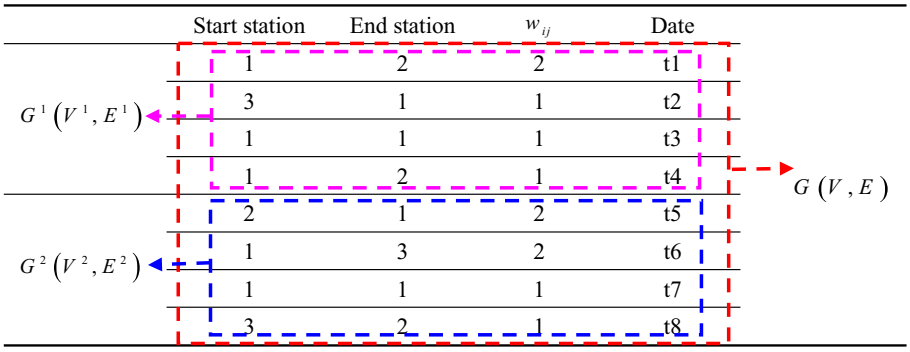

Table 2
Spatial-temporal characteristics parameters of green travel behavior.

		0:00–6:00	6:00–7:00	7:00–10:00	10:00–17:00	17:00–20:00	20:00–24:00
B-PBN	Δt^{α}	120 min	5min	2min	2.5min	1min	5min
	c_1	0.60	0.63	0.60	0.66	0.65	0.68
R-PBN	Δt^{α}	120 min	5min	1min	2.5min	1min	5min
	c_2	0.61	0.67	0.63	0.66	0.71	0.66

method to describe the node flow by dominant directional component in the vector, and construct directional degree index to describe the spatial characteristics of green travel behavior. Then, the indicators and methods for calculating the time-varying of green travel behavior are established by temporal network.

At last, based on the real-time travel data from 2017/03/20–2017/03/26 in Nanjing public bike company, we conducted the empirical analysis, and find green travel behavior of borrowing public bike and returning public bike are highly time-varying, which need to be studied separately in six different time intervals. We find that although the above two green travel behaviors have differences in spatial characteristics, the temporal characteristics are the same. That is, the above two green travel behaviors can be analyzed within the same temporal windows. Therefore, the analysis method of green travel behavior proposed in this paper opens up a new horizon for the research of the dynamic rebalancing.

Limited by the data, we only focus on green travel behavior between March 20 and March 27, 2017, its spatial-temporal characteristics are inevitably not comprehensive and profound. Although each day is divided into six periods by spatial-temporal characteristics of green travel behavior, the intervals of temporal window in each period are still artificially equal. In the future, we will establish a new temporal window, in which the intervals

change in real time with green travel behavior.

Acknowledgements

The Research was supported by the following foundations: The National Natural Science Foundation of China (71690242, 71503132, 51876081, 71774077), Qing Lan Project of Jiangsu Province (SJ201812), Jiangsu Key Lab for NSLSCS (201904) and Soft science project of Taizhou (SRK20180041). Postgraduate & Practice Innovation Program of Jiangsu Province (KYCX18_023).

References

Ahmadreza, F.I., Robert, H., Lavanya, M., Naveen, E., 2017. An empirical analysis of public bike sharing usage and rebalancing: evidence from Barcelona and Seville. Transp. Res. A 97, 177–191.
Almaas, E., Kovács, B., Vicsek, T., Oltvai, Z.N., Barabási, A.L., 2004. Global organization of metabolic fluxes in the bacterium Escherichia coli. Nature 427 (6977), 839–843.
Benchimol, M., Benchimol, P., Chappert, B., de la Taille, A., Laroche, F., Meunier, F., Robinet, L., 2011. Balancing the stations of a self service "public bike hire" system. RAIRO-Oper. Res. 45 (1), 37–61.
Bordagaray, M., Dell'Olio, L., Fonzone, A., Ibeas, A., 2016. Capturing the conditions that introduce systematic variation in public bike-sharing travel behavior using data mining techniques. Transp. Res. Part C 71, 231–248.
Boss, D., Nelson, T., Winters, M., Ferster, C.J., 2018. Using crowdsourced data to monitor change in spatial patterns of public bike ridership. J. Transp. Health 9, 226–233.
Bullock, C., Brereton, F., Bailey, S., 2017. The economic contribution of public bike-share to the sustainability and efficient functioning of cities. Sustain. Cities Soc. 28, 76–87.
Chardon, C.M.D., Caruso, G., Thomas, I., 2016. Public bike-share rebalancing strategies, patterns, and purpose. J. Transp. Geogr. 55, 22–39.
Chardon, C.M.D., Caruso, G., Thomas, I., 2017. Public bike sharing system 'success' determinants. Transp. Res. Part A Policy Pract 100, 202–214.
Chemla, D., Meunier, F., Wolfler Calvo, R., 2013. Public bike sharing systems: solving the static rebalancing problem. Discr. Optim 10 (2), 120–146.
Contardo, C., Morency, C., Rousseau, L.M., 2012. Balancing a dynamic public public bike sharing system. In: Technical Report CIRRELT-2012-09, Montreal, Canada.
Dell'Amico, M., Hadjicostantinou, E., Iori, M., Novellani, S., 2014. The public bike sharing rebalancing problem: mathematical formulations and benchmark instances. Omega 45, 7–19.
Dong, G.G., Gao, J.X., Tian, L.X., Du, R.J., He, Y.H., 2012. Percolation of partially interdependent networks under targeted attack. Phys. Rev. E 85, 016112.
Dong, G.G., Fan, J., Shekhtman, L.M., Saray, S., Tian, L.X., Stanly, H.E., Havlin, S., 2018. 2018. Resilience of networks with community structure behaves as if under an external field. Proc. Natl. Acad. Sci. Unit. States Am. 201801588, SCI.
Fishman, E., Washington, S., Haworth, N., 2012. Barriers and facilitators to public public bike scheme use: a qualitative approach. Transport. Res. F Traffic Psychol. Behav. 15, 686–698.
Fishman, E., Washington, S., Haworth, N., Watson, A., 2014. Factors influencing public bike share membership: an analysis of Melbourne and Brisbane. Transp. Res. Part A Policy Pract 71, 17–30.
Fuller, D., Gauvin, L., Kestens, Y., Morency, P., Drouin, L., 2013. The potential modal shift and health benefits of implementing a public public bike share program in Montreal, Canada. Int. J. Behav. Nutr. Phys. Act 10, 2–7.
Godavarthy, R.P., Taleqani, A.R., 2017. Winter public bikesharing in US: user willingness, and operator's challenges and best practices. Sustain. Cities Soc. 30, 254–262.
Graves, J.M., Pless, B., Moore, L., Nathens, A.B., Hunte, G., Rivara, F.P., 2014. Public public bike share programs and head injuries. Am. J. Public Health 104, 106–111.
Haider, Z., Nikolaev, A., Kang, J.E., Kwon, C., 2018. Inventory rebalancing through pricing in public public bike sharing systems. Eur. J. Oper. Res. 270, 103–117.
Hamilton, T.L., Wichman, C.J., 2018. Public bike infrastructure and traffic congestion: evidence from DC's Capital Public bikeshare. J. Environ. Econ. Manag. 87, 72–93.
Iderlina, M.B., Bean, R., Corcoran, J., Pojani, D., 2016. How does our natural and built environment affect the use of public bike sharing? Transp. Res. Part A Policy Pract 94, 295–307.
Jäppinen, S., Toivonen, T., Salonen, M., 2013. Modelling the potential effect of shared public bikes on public transport travel times in Greater Helsinki: an open data approach. Appl. Geogr. 43, 13–24.
Jensen, P., Rouquier, J.B., Ovtracht, N., Robardet, C., 2010. Characterizing the speed and paths of shared public bike use in Lyon. Transp. Res. Part D 15 (8), 522–524.
Kloimllner, C., Papazek, P., Hu, B., Raidl, G.R., 2014. Balancing public bike sharing systems: an approach for the dynamic case. In: Proceedings of European Conference on Evolutionary Computation in Combinatorial Optimization, pp. 73–84.
Liu, H.C., Lin, J.J., 2019. Associations of built environments with spatiotemporal patterns of public bicycle use. J. Transp. Geogr. 74, 299–312.
Mattson, J., Godavarthy, R., 2017. Public bike share in Fargo, North Dakota: keys to success and factors affecting ridership. Sustain. Cities Soc. 34, 174–182.
Pfrommer, J., Warrington, J., Schildbach, G., Morari, M., 2014. Dynamic vehicle redistribution and online price incentives in shared mobility systems. IEEE Trans. Intell. Transp. Syst. 15 (4), 1567–1578.
Pritcharda, J.P., Tomasiellob, D.B., Giannottib, M., Geursa, K., 2019. Potential impacts of bike-and-ride on job accessibility and spatial equity in São Paulo. Brazil. Transp. Res. Part A 121, 386–400.
Rainer-Harbach, M., Papazek, P., Raidl, G.R., Hu, B., Kloimüllner, C., 2015. PILOT, GRASP, and VNS approaches for the static balancing of public bike sharing systems. J. Glob. Optim. 1–33.
Ricci, M., 2015. Public bike sharing: a review of evidence on impacts and processes of implementation and operation. Res. Transp. Bus. Manag 15, 28–38.
Schuijbroek, J., Hampshire, R., van Hoeve, W.J., 2017. Inventory rebalancing and vehicle routing in public bike sharing systems. Eur. J. Oper. Res. 257 (3), 992–1004.
Shui, C.S., Szeto, W.Y., 2018. Dynamic green public bike repositioning problem- A hybrid rolling horizon artificial bee colony algorithm approach. Transp. Res. Part D 60, 119–136.
Si, H.Y., Shi, J.G., Wu, G.D., Chen, J.D., Zhao, X.B., 2019. Mapping the public bike sharing research published from 2010 to 2018: a scientometric review. J. Clean. Prod. 213, 415–427.
Szeto, W.Y., Liu, Y., Ho, S.C., 2016. Chemical reaction optimization for solving a static public bike repositioning problem. Transport. Res. Transport Environ. 47, 104–135.
Wang, J.H., Tsai, C.H., Lin, P.C., 2016. Applying spatial-temporal analysis and retail location theory to public public bikes site selection in Taipei. Transp. Res. Part A 94, 45–61.
Wang, M., Zhou, X., 2017. Public bike-sharing systems and congestion: evidence from US cities. J. Transp. Geogr. 65, 147–154.
Wang, M.G., Tian, L.X., Du, R.J., 2016a. Research on the interaction patterns among the global crude oil import dependency countries: a complex network approach. Appl. Energy 180, 779–791.
Wang, M.G., Chen, Y., Tian, L.X., Jiang, S.M., Tian, Z.H., Du, R.J., 2016b. Fluctuation behavior analysis of international crude oil and gasoline price based on complex network perspective. Appl. Energy 175, 109–127.
Wang, M.G., Tian, L.X., Zhou, P., 2018. A novel approach for oil price forecasting based on data fluctuation network. Energy Econ. 71, 201–212.
Zhang, D., Yu, C.H., Desai, J., Lau, H.Y.K., 2017. Sandeep Srivathsan A time-space network flow approach to dynamic repositioning in public bike sharing systems. Transp. Res. Part B 103, 188–207.
Zhang, Y., Brussel, M.J.G., Thomas, T., Maarseveen, M.F.A.M., 2018. Mining public bike-sharing travel behavior data: an investigation into trip chains and transition activities. Comput. Environ. Urban Syst. 69, 39–50.
Zhao, J., Wang, J., Deng, W., 2015. Exploring public bike-sharing travel time and trip chain by gender and day of the week. Transp. Res. Part C 58, 251–264.